INTL JOURNAL OF ELECTRONICS AND TELECOMMUNICATIONS, 2019, VOL. 65, NO. 4, PP. 611–617
Manuscript received March 31, 2019; revised September, 2019. DOI: 10.24425/ijet.2019.129820

Characterizing The SINR in Poisson Network Using Factorial Moment

Moubachir Madani Fadoul, Razali Ngah, and Alireza Moradi

***Abstract*—Usually, cellular networks are modeled by placing each tier (e.g macro, pico and relay nodes) deterministically on a grid. When calculating the metric performances such as coverage probability, these networks are idealized for not considering the interference. Overcoming such limitation by realistic models is much appreciated. This paper considered two- tier two-hop cellular network, each tier is consisting of two-hop relay transmission, relay nodes are relaying the message to the users that are in the cell edge. In addition, the locations of the relays, base stations (BSs), and users nodes are modeled as a point process on the plane to study the two hop downlink performance. Then, we obtain a tractable model for the k-coverage probability for the heterogeneous network consisting of the two-tier network. Stochastic geometry and point process theory have deployed to investigate the proposed two-hop scheme. The obtained results demonstrate the effectiveness and analytical tractability to study the heterogeneous performance.**

***Keywords*—Heterogeneous network, stochastic geometry, factorial moment, coverage probability**

I. Introduction

AS a variety of infrastructure is being deployed including pico, macro and femto BSs [1], as well as xed relay stations [2], the deployment of the cellular network is taking on a massively heterogeneous network (HetNet) character. Interference management is the main challenge in deploying heterogeneous cellular networks. Some challenges have occurred in high dense network such as less coverage, cost, co-channel, and intercell interference due to an increase in the number of connected devices [3]. Hence, the resulting interference is also becoming more complicated.

The denser nature of cellular networks makes them increasingly irregular [4]. This depicts small cells that opportunistically deployed in hot-spots, and hence highly irregular. As a result in current and future deployments, the popular deterministic grid model (see Fig. 1) is increasingly anachronistic. Even for single-tier networks, the grid model is quite idealized and a perturbed grid model is sometimes used for macrocell locations [2], [5]. A random spatial model will often be a more appropriate model than the deterministic one in characterizing the HetNet. Among the random spacial models that modeling the BS locations by a two-dimensional point process, the Poisson Point Process (PPP) is being the simplest model [6], [7].

However, cellular networks are modeled the BSs usually by arranging them on a line or circle as in the Wyner model or placing them on a grid (with a regular shape), with the user and relay are either randomly or deterministically distributed across the network to calculate the signal-to-interference-and-noise ratio (SINR). The resulting SINR consists of multiple random complex variables. Thus, this did not capture the randomness in the the inter-cell interference [8] and cellular network distribution. These models are not tractable because they are highly idealized, thus to evaluate the outage/success probability and ergodic capacity, complex system level simulation is used. SINR closed-form using stochastic geometry were derived, to reduce the dependence on simulations [2], [9].

It is obvious that, the Wyner and grid models are not practicable for characterizing the SINR, stochastic geometry has risen as a powerful tool to quantify and model the success probability and interference in cellular networks which approximates the actual networks [6]. To provide insightfullness into the operation of the network in the form of scaling laws, Poisson point processes (PPP) model is applied. The sign of PPP model is constituted of BS, relay and user parameters (e.g. transmit power and path-loss exponent). Under a homogeneity condition, it recently shown that, the BS positions are agnostic to the radio propagation waves, this mimics the BSs PPP distribution [10], [11]. Some metric performance computation such as the coverage probability [7], [12], with its lower and upper bound derivations [7], [13]. Reference [14], [15] study the effect of for two-tier networks with the effect of channel uncertainty. In two tier network, [16] compares single and multiuser performance. A comprehensive analysis of the performance metrics like coverage probability is computed by averaging over all cell sizes and scenarios [6] while the extension to multi-tier is studied in [17]. However, the challenge in previous work is incorporating heterogeneous infrastructure like fixed relays into the system model.

This paper, however, characterizes the randomly distributed performance of two-tier network by using a stochastic geometry tool to derive bounds for the coverage probability. Finally, numerical results include grid model as baseline scheme to validates the analytical findings.

Next, Section II, depicts the system model along with the SINR characterization by using the factorial moment to derive the coverage probability for single-tier and multi-tier network. In Subsection III-A the coverage probability is derived. Section

The authors would like to express their gratitude to Ministry of Higher Education (MOHE) in Malaysia and Universiti Teknologi Malaysia (UTM) for providing the financial support for this research through the Fundamental Research Grant Scheme (FRGS) (R. J130000.7823.4F965). The Grant is managed by Research Management Centre (RMC) at UTM.

The Authors are with the Wireless Communication Centre, Universiti Teknologi Malaysia, Johor Bahru, Skudai (e-mail: mfmoubachir2@live.utm.my).

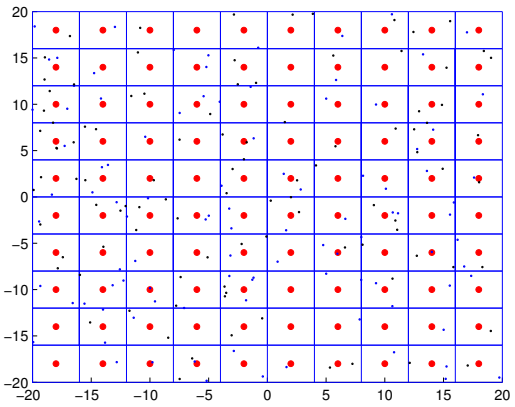

Fig. 1. The grid cellular network topology, where every Voronoi cell represents tier's coverage area - distributed as PPP where the black circle represents tier-1, blue dot represents tier-2 and the black circle represents tier-3

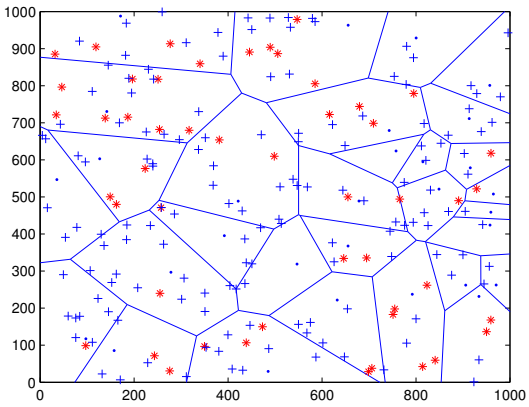

Fig. 3. The Voronoi multi-tier topology, where each Voronoi cell is the coverage area of a tier - distributed as PPP where the blue plus sign represent tier-1, red star represents tier-2 and the blue dot represent the tier-3

IV offers the numerical results, and Section V offers the conclusion.

II. Heterogeneous Cellular Network Model

In multi-tier heterogeneous assisted relay network, consider multiple independent dual-hop relaying system Fig. 2.

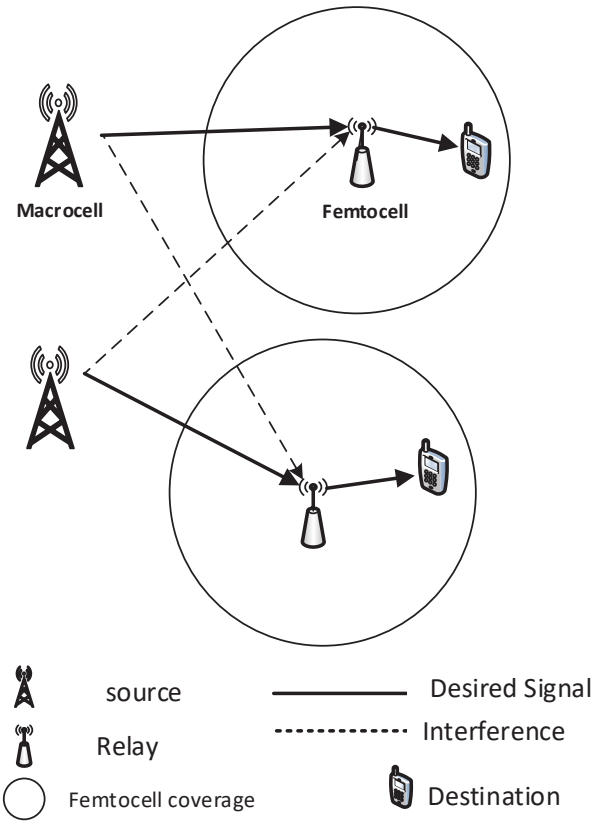

Fig. 2. Cellular relay network, in which three-tier network consisting of macro, pico and femtocells network with intended signal and interferences across tiers are shown. Solid lines depict the desired signal, and the dashed lines depict interference

The BSs constitute a Voronoi tessellation of the plane (see Fig. 3). The communication between user and BS occurs through the relay in the Voronoi cell. To examine what the network perceives, the BSs are located at the origin. On $\mathbb{R}^3$, the BSs, and relays are modeled with a stationary Poisson point process or homogeneous $\Phi_1 = \{X_1\}$ with density λ_1, and $\Phi_2 = \{X_2\}$ with density λ_2 respectively. The deterministic pathloss function for SR and RD hops is defined by

Each BSs-tier differs for each user in the target SIR β_k, number of antennas M_k, the deployment density λ_k, and the transmitted power P_k. These BS-tiers are modeled by an independent and homogeneous Poisson Point Process (PPP) Φ_k with density λ_k. Such claim under sufficient channel randomness by theoretical arguments and empirical observations [18] is validated to be accurate for the multi-tiers network. To simplify the analysis, we ignore the thermal noise in some scenarios as cellular networks are proven to be interference-limited [19].

A. Channel Model

A typical single-antenna relay/user located at the origin and associated with the closest BS in the downlink. According to Silvnyak's theorem [20], users in the Voronoi cell of a BS are associated with it, resulting in a coverage areas that comprise a Voronoi tesselation on the plane, as depicted in Fig. 3. A traditional grid model uniformly places the BSs at the center of the hexagonal model as shown in Fig. 1, and it is evaluated via simulations because it does not lead to a tractable model.

Let us define the deterministic path-loss function for SR and RD hops as follows

$$\ell\left(\mid x \mid\right) = \left(K \mid x \mid\right)^{\beta}, \tag{1}$$

where $\beta > 2$ denotes the path-loss exponent and the path-loss constant $K > 0$. Let S_X denotes the propagation effects such as shadowing with mean $\mathbb{E}[S_x] = 1$ from the origin to X. The P_X is representing the signal power that emitting from the BS at X, let $\{(S_X, P_X)\}_{X\in\Phi} \subset \mathbb{R}^+$ is equal distribution to (S, P) be independent positive random vectors that constitute

X.

Modifying references [21] [22] and [23] to suit our system model, we consider the propagation loss of the Poisson process on $\mathbb{R}^+$ for SR hop and RD hop respectively given as

$$\Theta_u = Y_u = \left\{ \frac{\ell_u \mid X_u \mid}{P_{Xu} S_{Xu}},\ X_u \in \Phi_u \right\}, \tag{2}$$

$$\Theta_k = Y_k = \left\{ \frac{\ell_k \mid X_k \mid}{P_{Xk} S_{Xk}},\ X_k \in \Phi_k \right\}, \tag{3}$$

Lemma1 : from the random location of nodes and the randomness of fading as in [19] and applying the mapping theorem [24]. The effect of propagation loss Y is considered as a non-homogeneous Poisson point process on $\mathbb{R}^+$ with intensity measure $\Lambda([0,t)) = at^{\beta/2}$, where the propagation constant is

$$a = \frac{\lambda \pi \mathbb{E}\left[(PS)^{\frac{2}{\beta}}\right]}{K^2} \tag{4}$$

Despite the distribution of S being arbitrary, we assume that $\mathbb{E}\left[S^{\frac{2}{\beta}}\right] < \infty$[1].

Proof : for given Φ_u and Φ_k, apply the displacement theorem for Poisson point process [25]-Theorem 1.3.9, Θ_u and Θ_k constitute a non homogeneous point process on $\mathbb{R}^+ = [0,\infty)$ of intensity measure Λ as follows

$$\begin{aligned}
\Lambda([0,s]) &= \mathbb{E}[\Theta([0,s])] \\
&= \lambda \int_{\mathbb{R}^2} Pr\{\ell(\mid z \mid)/S \le s\} dz \\
&= 2\pi\lambda \int_0^\infty \mathrm{xPr}\{\ell(\mid \mathrm{z} \mid)/\mathrm{S} \le \mathrm{s}\}\mathrm{dx} \\
&= 2\pi\lambda \int_0^\infty \mathrm{x}\mathbb{E}[1\{\ell(\mid \mathrm{z} \mid)/\mathrm{S} \le \mathrm{s}\}\mathrm{dx} \\
&= 2\pi\lambda \mathbb{E}\left[\int_0^{(\mathrm{sS})^{1/\beta}/\mathrm{K}} \mathrm{xdx}\right] \\
&= \frac{\lambda\pi s^{2/\beta}}{K^2}\mathbb{E}\left[S^{2/\beta}\right].
\end{aligned}$$

B. SINR Charaterization

The signal-to-interference-plus-noise ratio (SINR) for the SR hop and RD hop is formulated, which allows us to analyze the coverage probability.

The SR hop's SINR of the positive $\mathbb{R}^+$ for a relay defined as

$$\mathrm{SINR_k(X)} \triangleq \frac{\mathrm{F}_{x_k}\mathrm{Y_k^{-1}}}{\sigma_k + \mathrm{I}_k - \mathrm{Y}_k^{-1}\mathrm{F}_{x_k}}, \mathrm{I_k} = \sum_{\mathrm{Y_k}\in\Theta_\mathrm{k}} \mathrm{Y_k^{-1}F_{x_k}}, \tag{5}$$

with an additive white noise power $\sigma_\mathrm{k} \ge 0$ and $\mathrm{I_k}$ is the power received from other nodes, $\{F\}_{X\in\Phi}$ denotes the Rayleigh fading for the two hops with $\mathbf{E}[F_x] = 1$. The term $(\mathrm{I_k} - \mathrm{Y_k^{-1}}F_{x_k})$ captures the interference that the relay node experienced. While the RD hop's SINR of a user with an additive white noise power $\sigma_u \ge 0$ given as

$$\mathrm{SINR_u(X)} \triangleq \frac{\mathrm{Y_u^{-1}F_{x_u}}}{\sigma_\mathrm{u} + \mathrm{I_u} - \mathrm{Y_u^{-1}F_{x_u}}}, \mathrm{I_u} = \sum_{\mathrm{Y_u}\in\Theta_\mathrm{u}} \mathrm{Y_u^{-1}F_{x_u}}, \tag{6}$$

where $\mathrm{I_u}$ is the power received from other nodes. The term $(\mathrm{I_u} - \mathrm{Y_u^{-1}F_{x_u}})$ is the interference that the user node experienced[2].

Further, the distribution of $\{Y^{-1}\}$ is an inhomogeneous Poisson point process with intensity $(2a/\beta)t^{-1-2/\beta}dt$.

III. SINR CHARACTERIZATION BY USING FACTORIAL MOMENT MEASURES

Two useful integrals are presented here for $x \ge 0$, the first one is the multi-coverage characteristics introduced without considering the effect of fading in [23]

$$\mathcal{I}_{n,\beta}(x) = \frac{2^n \int_0^\infty u^{2n-1} e^{-u^2 - u^\beta x \Gamma(1-2/\beta)^{-\beta/2}} du}{\beta^{n-1}(\bar{C}(\beta))^n (n-1)!}, \tag{7}$$

where

$$\bar{C}(\beta) = \frac{2\pi}{\beta sin(2\pi/\beta)} = \Gamma(1-2/\beta)\Gamma(1+2/\beta). \tag{8}$$

For simplification

$$\mathcal{I}_{n,\beta}(0) = \frac{2^{n-1}}{\beta^{n-1}(\bar{C}(\beta))^n}. \tag{9}$$

while the second one is integral over hyper-cube which is the generalization as shown by 10

$$\mathcal{J}_{n,\beta}(x_1,...,x_n) = \frac{(1+\sum_{j=1}^n x_j)}{n} \int\limits_{[0,1]^{n-1}} \frac{\prod_{i=1}^{n-1} v_i^{i(2/\beta+1)-1}(1-v_i)^{2/\beta}}{\prod_{i=1}^n (x_i+\eta_i)} dv_1...dv_{n-1}, \tag{10}$$

where

$$\begin{cases}
\eta_1 = & v_1 v_2 ... v_{n-1} \\
\eta_2 = & (1-v_1) v_2 ... v_{n-1} \\
\eta_3 = & (1-v_2) v_3 ... v_{n-1} \\
\cdots & \\
\eta_n = & 1 - v_{n-1}.
\end{cases} \tag{11}$$

[1]Note that $2/\beta < 1$ and using $\mathbb{E}[S] = 1 < \infty$, thus the propagation effect is bounded

[2]A similar approach for Nakagami-m fading and Rician fading is proposed in [26]

For further simplification, refer to Appendix.

A. $\mathcal{K}$-coverage probability by using Factorial Moment Measures

At the SINR level T, the distribution of the coverage number of the user, is defined as the number of either BSs and relays that the user can connect to, namely

$$\mathcal{N}(T) = \sum_{(Z,T)\in\tilde{\Psi}} \mathbf{1}[\mathrm{Z} > \mathrm{T}]. \tag{12}$$

The probability that a relay is connecting to at least one of BSs in the network is known as the $\mathcal{K}$-coverage probability, as below

$$\mathcal{P}^{(k)} = \mathbf{P}\{\mathcal{N} \geq \mathrm{k}\}. \tag{13}$$

The probability that a relay is connecting to at least one of BSs in the network is known as the $\mathcal{K}$-coverage probability, as below

$$\mathcal{P}^{(k)} = \mathbf{P}\{\mathcal{N} \geq \mathrm{k}\}. \tag{14}$$

for any $n \geq 1$ and given T, the nth symmetric sum can be given by

$$S_n(\mathrm{T}) = \mathbb{E}\left[\sum_{x_1,\ldots,x_n\in\tilde{\Psi}} \mathbf{1}(\mathrm{Z_i}) > \mathrm{T_i},\ i = 1,...,n \mid \Phi\right], \tag{15}$$

where for a given Φ, the conditional probability is denoted by $\mathbf{P}\{... \mid \Phi\}$. Use $S_0(\mathrm{T}) = 1$, and for a given $\mathcal{N}(\mathrm{T})$ BSs, the expected number of ways that the relay can choose from n BSs to connect with for $\mathrm{SINR} > \mathrm{T}$, is denoted by $S_n(\mathrm{T})$. The following Lemma is related to the famous inclusion-exclusion principle [27].

Lemma 2 : for $\mathcal{K} \geq 1$ we obtain

$$\mathcal{P}^{(k)}(\mathrm{T}) = \sum_{n=k}^{\infty}(-1)^{n-k}\binom{n-1}{k-1} S_n(\mathrm{T}), \tag{16}$$

$$\mathbf{P}\{\mathcal{N}(\mathrm{T}) = k\} = \sum_{n=k}^{\infty}(-1)^{n-k}\binom{n}{k} S_n(\mathrm{T}), \tag{17}$$

$$\mathbb{E}[z^{\mathcal{N}(\mathrm{T})}] = \sum_{n=k}^{\infty}(z-1)^n S_n(\mathrm{T}),\ z \in [0,1], \mathbb{E}[\mathcal{N}(\mathrm{T})] = S_1(\mathrm{T}). \tag{18}$$

The right-hand side of the above equation, contains our quantities of interest, which will be evaluated later. Before that, in the following section we evaluate the symmetric sums $S_n(\mathrm{T})$, and observes that the infinite summations in the above expressions reduce to finite sums under reasonable conditions ($S_n(\mathrm{T}) = 0$ for n large enough).

B. Multi-tier network by using Factorial Moment Measures

In a heterogeneous network, we examine the multi-tier network for $\mathcal{K}$-coverage probability and the SINR threshold T which depends only on the BS tier which could be the BS or relay. For a given m-tier of BSs/relays that independently homogeneous Poisson point process $\{\Phi_j\}$ with densities $\{\lambda_j\}$ we have

$$\tilde{\Phi}_j = \{(X_j, (S_{X_j}, P_{X_j}, \tau_j))\}. \tag{19}$$

The propagation effect and the BS's power depends on the tier, and the SINR threshold is changed to non-random such that

$$\mathbb{E}[(P_j S_j)^{2/\beta}] < \infty, \quad j = 1, ..., m. \tag{20}$$

for $j \neq k$, the path-loss parameters β and K for the network given that

$$\lambda_j^* = \lambda_j \mathbb{E}[(P_j S_j)^{2/\beta}]. \tag{21}$$

For the m-tier network $\tilde{\Phi} = \bigcup_{j=1}^{m} \tilde{\Phi}_j$.

Corollary 2 : for single tier network $\tilde{\Phi}^*$ with path-loss constant $K = 1$ and path-loss exponent α, such that $P^* = 1$, $S^* = 1$ and the BS/relay density

$$\lambda^*\lambda^* = \sum\nolimits_{j=1}^{m} \lambda_j^*, \tag{22}$$

given that T^* is distributed by

$$P(T^* = \tau_j) = \frac{\lambda_j^*}{\lambda^*}, \qquad j = 1, ..., m. \tag{23}$$

Proof : for each j tier $\tilde{\Phi}_j$, there is $\tilde{\Phi}_j^*$ as an equivalent tier, setting $P_j = 1$, $S_j = 1$ and density λ_j^*. From **Corollary 1**, applying the superposition theorem [28] we end this proof.

C. Single-tier network by using Factorial Moment Measures

For a single-tier with stationary Poisson point $\Phi = \{X\}$ and density λ, given a SINR threshold τ, the $\mathcal{K}$-coverage probability is derived in [23]. Where by the case $(\tau \geq 1)$ is considered as a special case of [7]-Theorem 1.

Corollary 3 : for single tier network, the condition $\mathbb{E}[(PS)^{2/\beta}] < \infty$ hold, then

$$S_n = S_n(\tau) = \tau_n^{-2n/\beta}\mathcal{I}_{n,\beta}((\sigma/\gamma)a^{-\beta/2})\mathcal{J}_{n,\beta}(\tau_n), \tag{24}$$

for $S_n = 0$ and $0 < \tau < 1/(n-1)$, where a is shown in (4) and τ_n is given by

$$\tau_n = \tau_n(\tau) = \frac{\tau}{1-(n-1)\tau}, \tag{25}$$

Therefore, the k-coverage probability is given by 26

$$\mathcal{P}^{(k)} = \mathcal{P}^{(k)}(\tau) = \sum\nolimits_{n=k}^{\lceil 1/\tau\rceil}(-1)^{n-k}\binom{n-1}{k-1}\tau_n^{-2n/\beta} \times \mathcal{I}_{n,\beta}((\sigma)a^{-\beta/2})\mathcal{J}_{n,\beta}(\tau_n), \tag{26}$$

For $T \geq 1$ and $k = 1$ the above expression reduces to a single-tier network [7]-eq. (2), when $\lceil 1/(\tau) \rceil = 1$ and $\tau \geq 1$ the above expression simplifies to

$$\mathcal{P}^{(1)}(\tau) = \frac{2(\tau)^{-2/\beta}}{\Gamma(1+\frac{2}{\beta})} \int_0^{\infty} u e^{-u^2\Gamma(1-2/\beta)-\sigma a^{-\beta/2}u^{\beta}} du. \quad (27)$$

IV. Numerical Results

The simulation and the theoretical procedure for the proposed system analysis are validated in this section as similar to [7] [29]. The $\mathcal{K}$ independent PPPs are generated with the given densities. The serving user is assumed to lie in the origin with $\beta_k = 0$ dB. A user is said to be in coverage if the target SIR from the BS is greater than the target.

In an interference-limited scenario ($\sigma = 0$), we set $K = 1$, $PS = 1$, unlike the multi-tier network where λ and P will be specified. To validate our analytical result, we generate our network simulation based on a circular region of radius 10 length units, and 10^5 as the number of network simulation. The path-loss exponent is assumed to be $\beta = 3$ and 5. The shadowing is modeled by a log-normal random variable with expectation 1 and 10 dB logarithmic standard deviation. If a user is able to connect to at least one BS with SINR above its threshold, the user is declared to be in coverage. Precisely, the coverage probability is the complementary cumulative function (CCDF) of the effective SINR, when SINR threshold is equal across all the tiers.

For a single tier-network, the $\mathcal{K}$-coverage probability $\mathcal{P}^{(k)}(\tau)$ for $\mathcal{K} = 1, 2, 3$ with $\beta = 3$ and $\beta = 5$, as in Fig. (4) and (5) respectively. This reminds us that, the kth strongest signal is related to the coverage probability by the tail distribution function of the SINR.

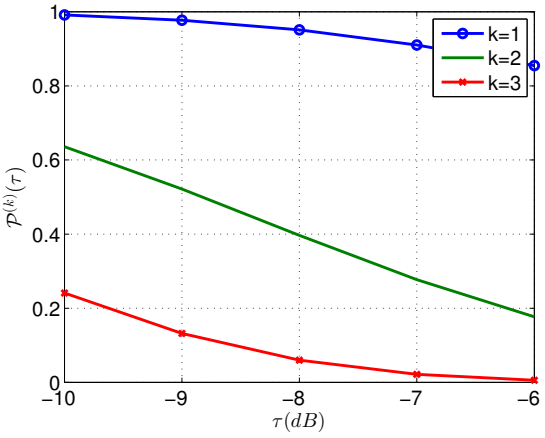

Fig. 4. For a single-tier network, k-coverage probability $P^{(k)}(\tau)$ for $\beta = 3$

Fig.6 shows the single-tier coverage probability [23] extended to a two-tier coverage probability network, which leads to SINR derivation for the heterogeneous network, where each tier has the same SINR thresholds. Clearly, the single-tier coverage probability is much smaller than the two-tier coverage probability, mainly when the single-tier and two-tier network are located nearby high power BSs. These results are performance equivalent.

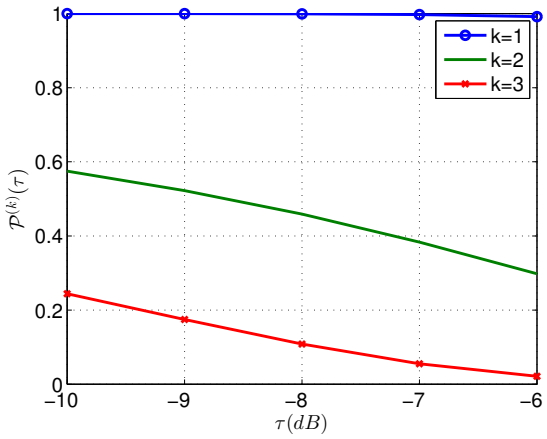

Fig. 5. For a single-tier network, $\mathcal{K}$-coverage probability $P^{(k)}(\tau)$ for $\beta = 5$

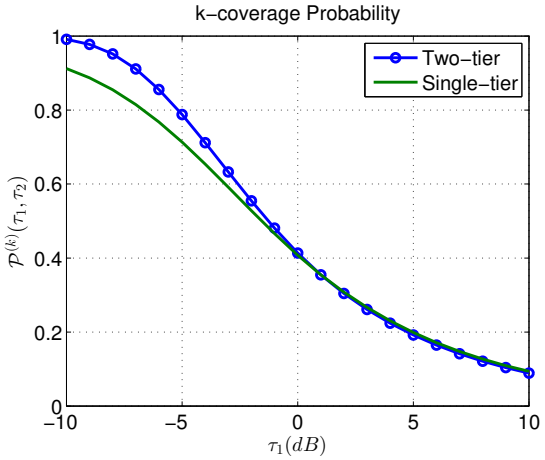

Fig. 6. For two-tier network, the 1-coverage probability $\mathcal{P}^{(1)}$ as function of τ_1 with $P_1 = 100P_2$,$\tau_2 = 1$dB, $\lambda_u = \lambda_k/2$ for $\beta = 3$ compared to a single-tier network

Fig. 7 shows that increasing τ, decreases the $\mathcal{K}$-coverage probability. It compares the random PPP model to the traditional grid model constituted by a Voronoi tessellation (see Fig. 1). The tier-1 distributed according to our PPP model, while tier-2 according to grid model. The grid model provides high coverage area across the whole SINR (upper bound). This is because the interference is dominant for the PPP model (lower bound). Since dense cellular networks are interference-limited due to the effect of noise, a gab has been observed when considering the $SNR = 10$ and $SNR \to \infty$. This validates the assumption that the noise can be ignored in interference-limited scenario.

V. Conclusion

The past few years experienced the use of random spatial models to investigate various aspects of heterogeneous network, it is strongly observed that most of these works focus on multi-tier or single-tier network. This paper studied the heterogeneous network, in which a tractable model to analyze the $\mathcal{K}$-tier coverage probability. The coverage probability is evaluated factorial moment measures of the point process

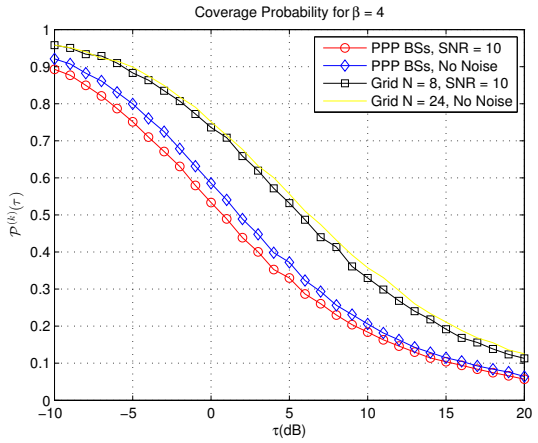

Fig. 7. k- Coverage probability comparison between grid model and our proposed PPP tier model with $\beta = 4$

formed by the SINR values perceived by the user. Where each tier differs in-terms of number of antenna, target Signal-to-Interference Ratio (SIR), transmitted power, and deployment density. To account for the fact that some transmission techniques provides higher coverage, we derive a $\mathcal{K}$-tier and single-tier transmission; by assuming that the BSs are located independently and to validate it's accuracy with the traditional grid model, an extensive comparison with the traditional grid model via numerical simulations was carried out.

REFERENCES

[1] V. Chandrasekhar, J. G. Andrews, and A. Gatherer, "Femtocell networks: a survey," vol. 46, no. 9, pp. 59–67, 2008.

[2] R. N. Romain Chevillon, Guillaume Andrieux and J.-F. Diouris, "Effects of directional antennas on outband d2d mmwave communications in heterogeneous networks," *International Journal of Electronics and Communications*, vol. 96, pp. 58–65, 2018.

[3] T. S. Rappaport, R. W. Heath Jr, R. C. Daniels, and J. N. Murdock, *Millimeter wave wireless communications*. Pearson Education, 2014.

[4] T. Shuminoski and T. Janevski, "5g terminals with multi-streaming features for real-time mobile broadband applications," *Radioengineering*, vol. 26, no. 2, p. 471, 2017.

[5] P. Mitran and C. Rosenberg, "On fractional frequency reuse in imperfect cellular grids," in *IEEE Wireless Commun. and Networking Conf. (WCNC)*. IEEE, 2012, pp. 2967–2972.

[6] J. G. Andrews, F. Baccelli, and R. K. Ganti, "A tractable approach to coverage and rate in cellular networks," *IEEE Trans. on Commun.*, vol. 59, no. 11, pp. 3122–3134, 2011.

[7] H. S. Dhillon, R. K. Ganti, F. Baccelli, and J. G. Andrews, "Modeling and analysis of k-tier downlink heterogeneous cellular networks," *IEEE Journal on Selected Areas in Communications*, vol. 30, no. 3, pp. 550–560, April 2012.

[8] R. Bhagavatula and R. W. Heath, "Adaptive bit partitioning for multicell intercell interference nulling with delayed limited feedback," vol. 59, no. 8, pp. 3824–3836, 2011.

[9] M. Haenggi, *Stochastic geometry for wireless networks*. Cambridge University Press, 2012.

[10] B. Błaszczyszyn, M. K. Karray, and H. P. Keeler, "Wireless networks appear poissonian due to strong shadowing," *IEEE Trans. Wireless Commun.*, vol. 14, no. 8, pp. 4379–4390, 2015.

[11] H. P. Keeler, N. Ross, and A. Xia, "When do wireless network signals appear poisson?" *arXiv preprint arXiv:1411.3757*, 2014.

[12] H. S. Dhillon, R. K. Ganti, and J. G. Andrews, "A tractable framework for coverage and outage in heterogeneous cellular networks," in *2011 Information Theory and Applications Workshop*. IEEE, 2011, pp. 1–6.

[13] H. S. Dhillon, M. Kountouris, and J. G. Andrews, "Downlink coverage probability in mimo hetnets," *Conference Record of the Forty Sixth Asilomar Conference on Signals, Systems and Computers*, pp. 683–687, 2012.

[14] S. Park, W. Seo, Y. Kim, S. Lim, and D. Hong, "Beam subset selection strategy for interference reduction in two-tier femtocell networks," vol. 9, no. 11, pp. 3440–3449, 2010.

[15] S. Park, W. Seo, S. Choi, and D. Hong, "A beamforming codebook restriction for cross-tier interference coordination in two-tier femtocell networks," vol. 60, no. 4, pp. 1651–1663, 2011.

[16] V. Chandrasekhar, M. Kountouris, and J. G. Andrews, "Coverage in multi-antenna two-tier networks," *IEEE Trans. Wireless Commun.*, vol. 8, no. 10, 2009.

[17] P. Madhusudhanan, J. G. Restrepo, Y. Liu, T. X. Brown, and K. R. Baker, "Multi-tier network performance analysis using a shotgun cellular system," in *Global Telecommun. Conf. (GLOBECOM 2011), 2011 IEEE*. IEEE, 2011, pp. 1–6.

[18] L. Zhou, F. Luan, S. Zhou, A. F. Molisch, and F. Tufvesson, "Geometry-based stochastic channel model for high-speed railway communications," *IEEE Transactions on Vehicular Technology*, vol. 68, no. 5, pp. 4353–4366, 2019.

[19] I. Trigui, S. Affes, and B. Liang, "Unified stochastic geometry modeling and analysis of cellular networks in los/nlos and shadowed fading," *IEEE Transactions on Communications*, vol. 65, no. 12, pp. 5470–5486, 2017.

[20] S. N. Chiu, D. Stoyan, W. S. Kendall, and J. Mecke, *Stochastic geometry and its applications*. John Wiley & Sons, 2013.

[21] Y. Liang and T. Li, "End-to-end throughput in multihop wireless networks with random relay deployment," *IEEE Transactions on Signal and Information Processing over Networks*, vol. 4, no. 3, pp. 613–625, 2018.

[22] B. Blaszczyszyn, M. K. Karray, and H. P. Keeler, "Using poisson processes to model lattice cellular networks," *2013 Proceedings IEEE INFOCOM*, pp. 773–781, 2013.

[23] H. P. Keeler, B. Blaszczyszyn, and M. K. Karray, "Sinr-based k-coverage probability in cellular networks with arbitrary shadowing," *2013 IEEE International Symposium on Information Theory*, pp. 1167–1171, 2013.

[24] M. Haenggi and R. K. Ganti, *Interference in large wireless networks*. Now Publishers Inc, 2009.

[25] F. Baccelli and B. Blaszczyszyn, *Stochastic geometry and wireless networks*. Now Publishers Inc, 2009, vol. 1.

[26] C. Liu and J. G. Andrews, "Multicast outage probability and transmission capacity of multihop wireless networks," *IEEE Trans. Inf. Theory*, vol. 57, no. 7, pp. 4344–4358, July 2011.

[27] H. U. Gerber, "Life insurance," in *Life Insurance Mathematics*. Springer, 1997, pp. 23–33.

[28] J. Kingman, "Poisson processes," *Oxford University Press*, 1993.

[29] B. Blaszczyszyn and H. P. Keeler, "Equivalence and comparison of heterogeneous cellular networks," *IEEE 24th International Symposium on Personal, Indoor and Mobile Radio Communications (PIMRC Workshops)*, pp. 153–157, 2013.

[30] F. Olver, D. Lozier, R. Boisvert, and C. Clark, "Digital library of mathematical functions, national institute of standards and technology," *dlmf. nist. gov/(release date 2011-07-01), Washington, DC*, 2010.

CONFLICT OF INTEREST

The author declares that they have no conflict of interest.

APPENDIX

Simplification on the integral $\mathcal{J}_{n,\beta}$

We further simplify the integral $\mathcal{J}_{n,\beta}(x_1, ..., x_n)$ as shown in (28). Use $n = 1$ the integral reduced to $\mathcal{J}_{1,\beta}(x_1) = 1$ and use $n = 2$ reduces the integral to (29). Further simplification leads to closed-form solution in (30),

$$\mathcal{J}_{n,\beta}(x_1, ..., x_n) = \frac{1}{n}\sum\nolimits_{j=1}^{n} \int\limits_{[0,1]^{n-1}} \frac{\prod_{i=1}^{n-1} v_i^{i(2/\beta+1)-1}(1-v_i)^{2/\beta}}{\prod_{i=1}^{n}(x_i+\eta_i)} dv_1 ... dv_{n-1}, \tag{28}$$

$$\mathcal{J}_{2,\beta}(x_1,x_2)=\frac{1}{2}\int_0^1 v_1^{2/\beta}(1-v_1)^{2/\beta}\left[\frac{1}{(x_1+v_1)}+\frac{1}{(x_2+1-v_2)}\right]dv_1. \tag{29}$$

$$\int_0^1 \frac{v^{2/\beta}(1-v)^{2/\beta}}{x+v}dv=\frac{1}{x}B(2/\beta+1,2/\beta+1)2^{F_1}(1,2/\beta+1;2(2/\beta+1);-1/x), \tag{30}$$

where 2^{F_1} is the hyper-geometric function [30]-Eq.15.6.1.